Molecular Crystals and Liquid Crystals

ISSN: 1542-1406 (Print) 1563-5287 (Online) Journal homepage: https://www.tandfonline.com/loi/gmcl20

Influences of He Contents and Panel Working Gas Pressures in Ternary Gas Mixture on Discharge Characteristics in AC Plasma Display Panel

Choon-Sang Park , Eun Young Jung & Heung-Sik Tae

To cite this article: Choon-Sang Park , Eun Young Jung & Heung-Sik Tae (2012) Influences of He Contents and Panel Working Gas Pressures in Ternary Gas Mixture on Discharge Characteristics in AC Plasma Display Panel, Molecular Crystals and Liquid Crystals, 564:1, 76-84, DOI: 10.1080/15421406.2012.691687

To link to this article: https://doi.org/10.1080/15421406.2012.691687

Published online: 20 Aug 2012.

Mol. Cryst. Liq. Cryst., Vol. 564: pp. 76–84, 2012

ISSN: 1542-1406 print/1563-5287 online
DOI: 10.1080/15421406.2012.691687

Taylor & Francis
Taylor & Francis Group

Influences of He Contents and Panel Working Gas Pressures in Ternary Gas Mixture on Discharge Characteristics in AC Plasma Display Panel

CHOON-SANG PARK,[1] EUN YOUNG JUNG,[2] AND HEUNG-SIK TAE[1,*]

[1]School of Electronics Engineering, College of IT Engineering, Kyungpook National University, Daegu 702-701, Korea
[2]Core Technology Lab., Corporate R&D Center, Samsung SDI Company Ltd., Cheonan, Chungcheongnam-Do 330-300, Korea

The discharge characteristics, particularly the address and sustain discharge characteristics, were examined relative to the He contents and panel working gas pressures under 11% Xe content in the 50-in. full HD AC-PDPs with a ternary gas mixture (Xe-He-Ne). The Xe content in this study was fixed at 11%. As the helium gas increases from 0 to 50%, the formative address delay becomes shortened by about 60 ns. In addition, the luminance are increased by about 15 cd/m^2 because of enlarging the Xe^{2*} excimer emission (823 nm) with an increase with the He gas. Also, the power consumption is reduced by about 30 W since the addition of He gas induces a reduction of cathode fall potential. The decrease in the gas pressure from 600 to 300 Torr causes a lower firing voltage, thereby resulting in reducing both the formative and statistical address delay times by about 71 ns and by about 65 ns, respectively. As a consequence, the pressure below 400 Torr and He content above 50% are the best panel factors suitable for high speed and low voltage driving of micro-discharge cells with the 50 in full HD cell size.

Keywords 50 in full-HD AC-PDP panel; pressure; high He; excimer emission; luminance; power consumption; firing voltage; formative address delay time; statistical address delay time; Vt closed curve

1. Introduction

Alternating-current plasma display panels (ac-PDPs) is one of the promising flat panel display devices with the sizes larger than 50 inch diagonal, and as such under very active development for its application to full high-definition television (FHD TV). However there remain still many problems such as the resolution, efficiency, driving voltage, lifetime, and discharge delay time that must be overcome urgently. Nowadays, some of the important issues are to speed-up the address time and to lower the driving voltage in full HD PDP. For the realization of the HD PDPs with high speed and high luminous efficiency, many researchers have so far studied on various parameters such as cell geometry [1,2], MgO [3], phosphor [4], gas composition [5–7], high Xe contents [8], driving waveform [9], and

*Address Correspondence to Prof. Heung-Sik Tae, School of Electronics Engineering, College of IT Engineering, Kyungpook National University, Sangyuk-dong, Buk-gu, Daegu 702-701, Korea (ROK). Tel: (+82)53-950-6563; Fax: (+82)53-950-5505. E-mail: hstae@ee.knu.ac.kr

sealing method [10]. However, electro-optical properties of gas conditions have not yet been studied, particularly for full HD PDPs with very small discharge cells. In particular, the role of He content in the ternary gas mixture has not been investigated in detail relative to the gas pressure in such a small discharge cell with full HD cell size.

Accordingly, this paper investigates intensively the influences of gas conditions, especially such as He concentration and gas pressure on the discharge characteristics, such as the address speed and power consumption in the 50 in full HD ac-PDPs with a ternary gas mixture (Xe-He-Ne).

2. Experimental Setup

Figure 1 shows the optical measurement systems and commercial 50 in full-HD test panel with three electrodes used in the experiments, where X is the sustain electrode, Y the scan electrode, and A the address electrode. The 50 in full-HD PDP modules are employed to examine the changes in the discharge characteristics relative to the gas conditions such as the He concentration and panel working gas pressure. The detailed panel specifications are listed in Table 1. The other specifications of all the test panels employed in this research were exactly the same, except for the He concentrations and panel working gas pressure. The Xe content in this study was fixed at 11%. The firing voltage was measured by using Vt closed curve analysis [11]. The firing voltage, $V_{f(xy)}$, is defined as the voltage that turns-on the first cell when applied between the X-Y electrodes. The address discharge delay time can be measured from the infrared emissions detected by the photo sensor. The address delay time is defined as a time elapsed from a 50% rise of the maximum scan pulse voltage level to a 99% reach of the peak emission signal measured by the oscilloscope. The brightness was measured with color analyzer (Minolta, CA-100+). Both visible and IR spectrum of PDP module were measured with using monochromator (Jovin Yvon Horiba, SPEX-1000M).

Figure 2 shows the applied driving waveforms, including the reset, address, and sustain periods. The frequency for the sustain period was 200 kHz. A driving method with a selective

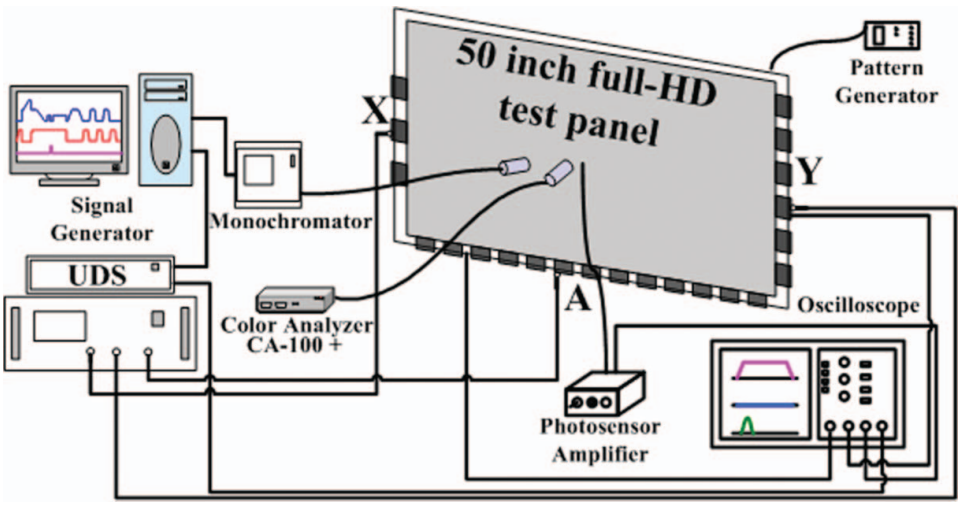

Figure 1. Schematic diagram of experimental setup employed in this paper.

Table 1. Specifications of 50 inch full-HD AC-PDP used in this study under various He contents (Ex.1) and panel working gas pressures (Ex.2)

Front Panel		Rear Panel	
ITO width	200 μm	Barrier rib width	50 μm
ITO gap	75 μm	Barrier rib height	120 μm
Bus width	70 μm	Address width	95 μm
Pixel pitch		576 μm $\times$ 576 μm	
Gas chemistry and Pressure	Ex.1	Ne-Xe (11%)-He (0, 35, 50%) -Pressure (420 Torr)	
	Ex.2	Ne-Xe (11%)-He (35%)- Pressure (100, 200, 300, 400, 500, 600 Torr)	
Barrier rib type		Closed rib	

Table 2. Optimal voltage levels of each period applied to test panels

		V_s	V_e	V_a	V_{set}	V_{scanh}	V_{scanl}
Ex.1	He 0%	200	110	65	390	−65	−185
	He 35%	200	110	65	390	−65	−185
	He 50%	210	110	65	400	−65	−185
Ex.2	100 Torr	200	95	65	390	−49	−174
	200 Torr	187	95	65	367	−55	−180
	300 Torr	188	95	65	373	−60	−185
	400 Torr	197	95	65	387	−65	−190
	500 Torr	213	95	65	408	−70	−195
	600 Torr	219	95	65	419	−75	−200

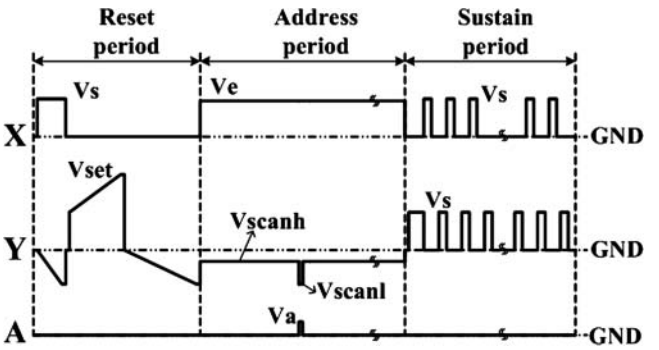

Figure 2. Schematic diagram of driving waveform used in this paper.

reset waveform was also adopted. The voltage levels in Fig. 2 were differently applied to each test panel because each test panel had different firing voltage conditions, as listed in Table 2.

3. Results and Discussion

3.1 Monitoring of Firing Voltage and Address Delay Time

Figure 3(a) shows the changes in the firing voltage, $V_{f(x\text{-}y)}$ measured by using Vt closed curve relative to He concentrations at 420 Torr. As shown in Fig. 3(a), the firing voltage was increased by about 15 V, when increasing the He content from 0 to 50%. The ion drift velocity is increased by increasing the He content, so that the resultant collision frequency is increased. The increase in the collision frequency results in decreasing the electron heating temperature [5–7,12]. Eventually, the firing voltage for breakdown is increased under the low electron heating temperature condition induced by increasing the He content.

Figure 3(b) shows the changes in the firing voltage, $V_{f(x\text{-}y)}$ measured by using Vt closed curve relative to the panel working gas pressures at He content of 35%. As shown in

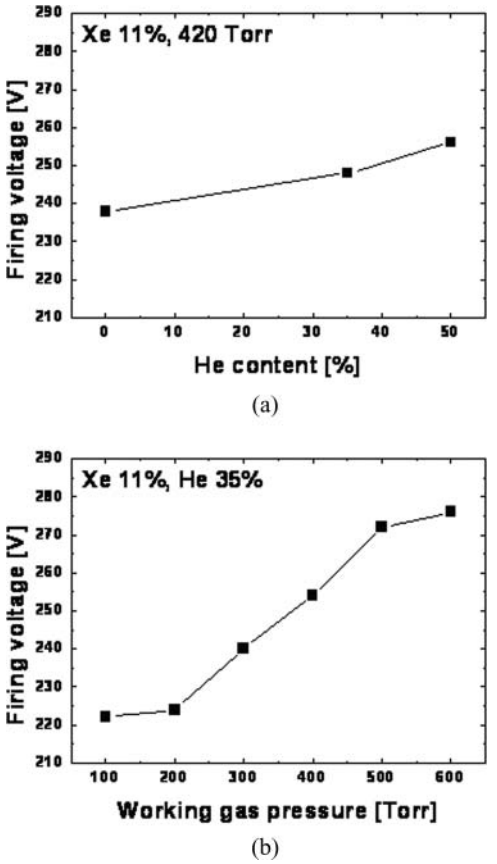

Figure 3. Comparison of firing voltage under various (a) He contents and (b) panel working gas pressures.

Fig. 3(b), the firing voltage considerably increased with an increase in the gas pressure. The gas pressure increase results in the decrease in the electron heating temperature because the mean free path is shortened and the collision probability is increased by increasing the gas pressure. Consequently, the firing voltage for discharge increased in case of increasing the gas pressure.

Figure 4(a) shows the changes in the address discharge delay characteristics under various He concentrations. As shown in Fig. 4(a), as the He gas partial pressure was increased, the formative address delay time (T_f) was observed to be decreased, whereas the statistical address delay time (T_s) was observed to be slightly increased. The formative address delay time depends on the ion drift velocity at an initial stage of discharge formation as the He atom increases. This ion drift velocity becomes lager with higher He atom concentration [5–7,12]. As a result, the high speed driving can be realized by adding to the He gas above 50%.

Figure 4(b) shows the changes in the address discharge delay characteristics under various panel working gas pressures. As shown in Fig. 4(a), as the gas pressure was

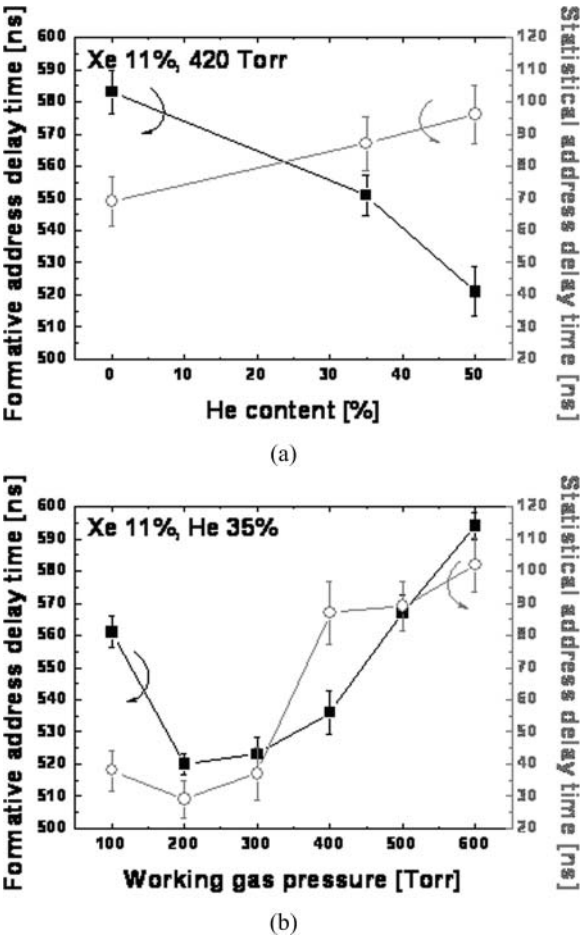

Figure 4. Comparison of formative and statistical address delay times under various (a) He contents and (b) panel working gas pressures.

decreased from 600 to 300 Torr, the T_f and T_s were observed to be considerably decreased. On the other hand, as the gas pressure was decreased from 200 to 100 Torr, the T_f and T_s were observed to be increased mainly due to the reduction of the ion drift velocity caused by increase in the collision probability with higher gas pressure. As a result, the high speed driving can be realized by decreasing the panel working gas pressure from 400 to 300 Torr.

3.2 Monitoring of Xe and Ne Emission Intensity

Figure 5 shows the relative infrared intensity of 823 and 828 nm when increasing the mixing ratio of He concentrations from 0 to 50%. With an increase in the He contents, the atomic emission of 828 nm decreased slightly, whereas the Xe^{2*} dimmer emission of 823 nm increased. With an increase in the He content, the high energy gain per unit electron is improved, thus resulting in enhancing the Xe-excitation efficiency by electrons [7]. Furthermore, the Ne emission of 585 nm was steeply reduced due to the decrease in the Ne contents, as shown in Fig. 5(a). Therefore, the emission intensity ratio of the Xe (823 and 828 nm) and to Ne (585 nm) emission was increased with an increase in the He concentration from 0 to 50%, as shown in Fig. 5(b).

Figure 6 shows the intensity ratio of the 823 and 828 nm to the 585 nm when increasing the gas pressure increases from 100 to 600 Torr. With an increase in the gas pressure, the

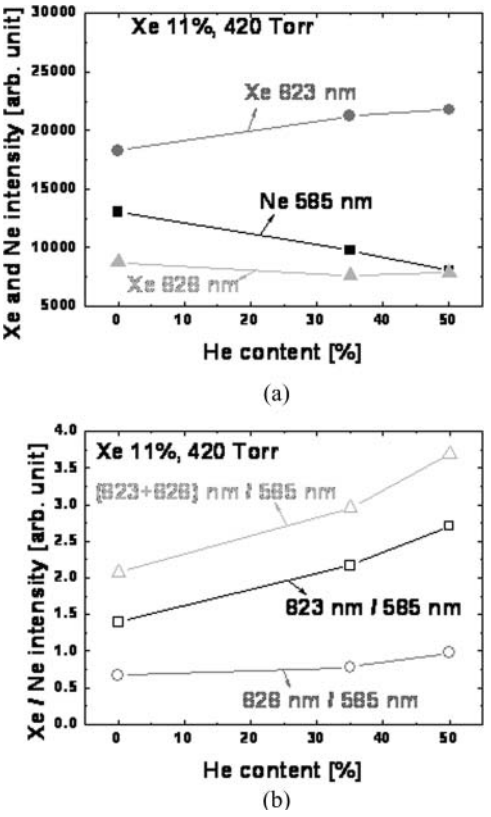

Figure 5. Comparison of (a) Xe (IR) and Ne spectral intensity and (b) Xe (IR)/Ne ratio under various He contents.

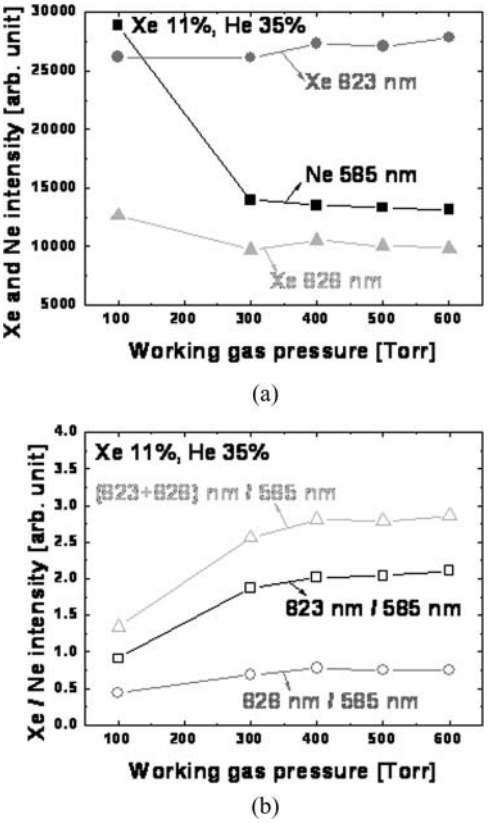

Figure 6. Comparison of (a) Xe (IR) and Ne spectral intensity and (b) Xe (IR)/Ne ratio under various panel working gas pressures.

atomic emission of 828 nm decreased, while the Xe^{2*} dimmer emission of 823 nm increased. Moreover, the Ne emission of 585 nm was reduced with an increase in the gas pressure, as shown in Fig. 6(a). The Ne emission was observed to be largely reduced from 100 to 300 Torr, meaning that the Ne ionization was largely reduced until 300 Torr presumably due to the decrease in the acceleration energy of electrons caused by increase in the collision probability. Therefore, the emission intensity ratio of the Xe to Ne emission increased, particularly, the emission intensity ratio of the Xe^{2*} dimmer of 823 nm to the Ne of 585 nm was considerably increased with an increase in the gas pressure, as shown in Fig. 6(b).

3.3 Monitoring of Luminance and Power Consumption

Figure 7(a) shows the changes in the luminance under full-white background and power consumption when increasing the He concentrations at Xe 11%. As the He concentrations increased from 0 to 50%, the luminance was increased by about 15 cd/m^2 because of enlarging the Xe^{2*} excimer emission of 823 nm, as shown in Fig. 5(a). In addition, the power consumption was decreased about 30 W since the cathode fall potential was reduced due to the reduction of the ions and electrons by adding the He gas [5–7,12]. As a result, the higher luminance and higher luminous efficacy was able to be obtained by adding the He gas.

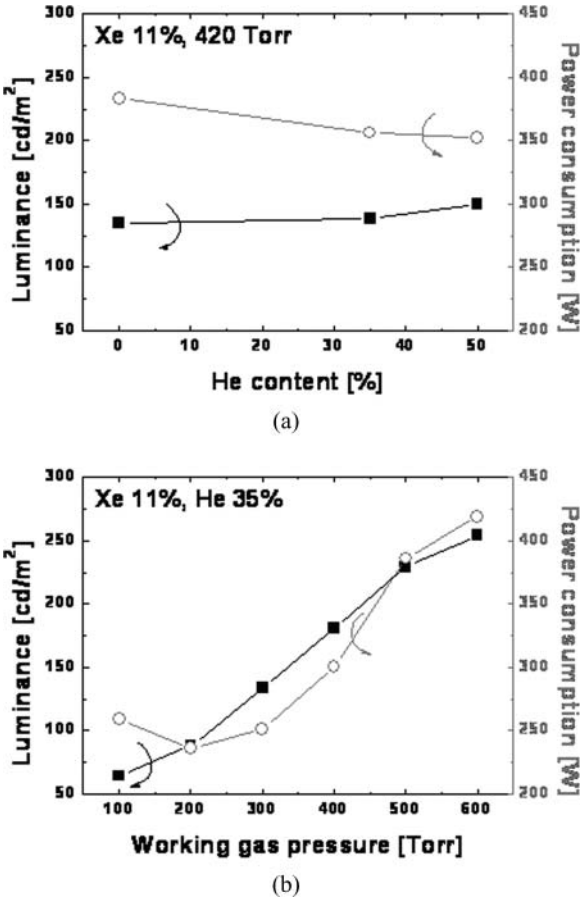

Figure 7. Comparison of luminance and power consumption under various (a) He contents and (b) panel working gas pressures.

Figure 7(b) shows the changes in the luminance under full-white background and power consumption when increasing the gas pressure from 100 to 600 Torr at Xe 11%. With an increase in the gas pressure, the luminance increases due to the Xe^{2*} excimer emission of 823 nm, as shown in Fig. 6(a). In addition, the power consumption was increased because of the firing voltage increasing in proportion to the gas pressure, as shown in Fig. 3(b). This experimental result on the gas pressure confirms that the optimal panel working gas pressure should be recommended to be a low pressure below 400 Torr, so as to realize the high speed and low driving voltage simultaneously.

Accordingly, it is concluded that the low pressure below 400 Torr and high He content above 50% contribute simultaneously to accelerating the address speed and lowering the driving voltage of the micro-discharge cells with the 50 in full-HD size.

4. Conclusion

This paper investigates the influences of the He contents and gas pressure on the discharge characteristics affecting the address speed and driving voltage conditions in the micro-discharge cells with the 50 in full-HD size. The paper illustrates the following experimental

results. First, the formative address delay becomes shortened about 60 ns when increasing the helium gas from 0 to 50%. Second, the luminance is increased by about 15 cd/m^2 when increasing the He concentration from 0 to 50%. In this case, the increase in the luminance is mainly due to the enlargement of the Xe^{2*} excimer emission. Third, the power consumption is decreased by about 30 W when increasing the He content. In this case, the reduction of the power consumption is chiefly due to the reduction of cathode fall potential induced by adding the He gas. Finally, the T_f and T_s are reduced by about 71 ns and 65 ns, respectively, when decreasing the gas pressure from 600 to 300 Torr. This phenomenon occurs as the firing voltage becomes lower with a decrease in the gas pressure. As a result, it is concluded that the low pressure below 400 Torr and the He content over 50% can realize the fast address and low drive voltage condition for the micro-discharge cell with the 50 inch full-HD size.

Acknowledgment

This work was supported in part by the Basic Science Research Program through the National Research Foundation of Korea (NRF) funded by the Korean Ministry of Education, Science and Technology (2012-0004506) and in part by Brain Korea 21 (BK21).

References

[1] Bae, H. S., Chung, W. J., & Whang, K. W. (2004). *J. Appl. Phys.*, *95*(1), 30–34.
[2] Chung, W. J., Seo, J. H., Jeong, D. C., & Whang, K. W. (2003). *IEEE Trans. Plasma Science*, *31*(5), 1023–1031.
[3] Uchida, G., Uchida, S., Akiyama, T., Kajiyama, H., & Shinoda, T. (2010). *J. Appl. Phys.*, *107*(10), 103311(1)–103311(7).
[4] Ozaki, I., Hori, N., Kawanami, Y., Okazaki, C., & Shiiki, M. (2003). *IDW'03*, *10*, 957–960.
[5] Uemura, N., Yajima, Y., Shibata, M., Kawanami, Y., & Namiki, F. (2003). *SID'03*, *34*, 784–787.
[6] Lee, I. S. & Choi, K. Y. (2006). *IEEE Trans. Plasma Science*, *34*(2), 360–370.
[7] Park, K.-H., Tae, H.-S., Hur, M., & Heo, E. G. (2009). *IEEE Trans. Plasma Science*, *37*(10), 2061–2067.
[8] Jung, H.-Y., Kim, T.-J., & & Whang, K. W. (2010). *IEEE Trans. Plasma Science*, *38*(4), 937–942.
[9] Park, H. D., Jang, S.-K., Kim, J. H., Tae, H.-S., & Chien, S.-I. (2011). *Jpn. J. Appl. Phys.*, *50*(10), 106202(1)–106202(5).
[10] Park, C.-S., Tae, H.-S., Kwon, Y.-K., & Heo, E. G. (2009). *Mol. Cryst. Liq. Cryst.*, *499*, 224–233.
[11] Tae, H.-S., Jang, S.-K., Cho, K.-D., & Park, K.-H. (2006). *IEEE Trans. Electron Devices*, *53*(2), 196–204.
[12] Lee, I. S., & Choi, K.-Y. (2005). *Jpn. J. Appl. Phys.*, *44*(8), 6230–6240.